Journal of Power Sources 242 (2013) 677–682

Contents lists available at SciVerse ScienceDirect

Journal of Power Sources

journal homepage: www.elsevier.com/locate/jpowsour

Short communication

Novel polymer electrolyte from poly(carbonate-ether) and lithium tetrafluoroborate for lithium–oxygen battery

Qi Lu, Yonggang Gao, Qiang Zhao, Ji Li, Xianhong Wang*, Fosong Wang

Key Laboratory of Polymer Eco-materials, Changchun Institute of Applied Chemistry, Chinese Academy of Sciences, Changchun 130022, PR China

HIGHLIGHTS

- Low-molecular weight poly(carbonate-ether) was prepared using zinc–cobalt double metal cyanide complex.
- Polymer electrolyte based on poly(carbonate-ether) and lithium tetrafluoroborate showed very high ionic conductivity.
- The properties of the polymer electrolyte were investigated by FT-IR, AFM and electrochemical measurements.
- The lithium–oxygen battery from this polymer electrolyte showed similar cyclic stability to traditional liquid electrolyte.

ARTICLE INFO

Article history:
Received 23 April 2013
Received in revised form
20 May 2013
Accepted 21 May 2013
Available online 6 June 2013

Keywords:
Polymer electrolyte
Lithium–oxygen battery
Poly(carbonate-ether)
Charge/discharge

ABSTRACT

Novel polymer electrolyte based on low-molecular weight poly(carbonate-ether) and lithium tetrafluoroborate has been prepared and used in lithium–oxygen battery for the first time, the electrolyte with approximate 17% of $LiBF_4$ showed ionic conductivity of 1.57 mS cm^{-1}. Infrared spectra analysis indicates that obvious interaction between the lithium ions and partial oxygen atoms in the host polymer exists, and the lithium salt and the host polymer have good miscibility. The lithium–oxygen battery from this polymer electrolyte shows similar cyclic stability to traditional liquid electrolyte observed by FT-IR, AFM and electrochemical measurements, which may provide a new choice for fabrication of all-solid-state high-capacity rechargeable lithium–oxygen battery with better safety.

1. Introduction

Lithium batteries, a class of chemical power sources utilizing different electrochemical processes of lithium element, are gaining dominant position in portable electronic applications, and showing great promise for the forthcoming new generation of pure electric vehicle applications [1–4]. As a novel member of this large family, lithium–oxygen battery (sometimes also called lithium–air battery) is becoming increasingly attractive due to its high theoretical energy density (>3400 Wh l^{-1}), proper cell voltage (≥3.0 V) and achievable environment-friendly components (heavy metal is unnecessary in both cathode and anode) [5–7]. Besides these, lithium–oxygen battery also has an obvious advantage shared by all types of metal–oxygen battery systems, namely, conveniently using the abundant oxygen resource in the air.

Currently, most research activities in lithium–oxygen battery focused on the exploitation of new cathode materials with ultra-high specific capacity, while less work related to solid electrolytes [8–11]. However, searching for suitable substitutes of traditional liquid electrolyte to construct all-solid-state battery is of crucial importance to improve battery safety for broader applications. Generally, the solid electrolytes can be divided into two major species according to the difference of the components, the inorganic solid electrolytes and the polymer electrolytes [12,13]. Polymer electrolytes are more suitable for most battery systems, since the inorganic solid analogues have relatively poor processability, and difficult to adjust with the volume change of battery electrode during charge–discharge processes.

A promising strategy to develop polymer electrolyte with higher ionic conductivity is to incorporate the plasticizing fragment like carbonate structure into the host polymer, such as poly(ethylene oxide) and poly(propylene oxide), to facilitate the mobility of polymer segment [14]. Poly(carbonate-ether) is a copolymer of carbon dioxide and epoxides [15,16], currently, poly(carbonate-ether) with different molecular weight, carbonate unit content and polymer backbone could be prepared conveniently by changes of the catalyst system, or adjusting copolymerization condition

* Corresponding author.
E-mail address: xhwang@ciac.jl.cn (X. Wang).

0378-7753/$ – see front matter © 2013 Elsevier B.V. All rights reserved.
http://dx.doi.org/10.1016/j.jpowsour.2013.05.095

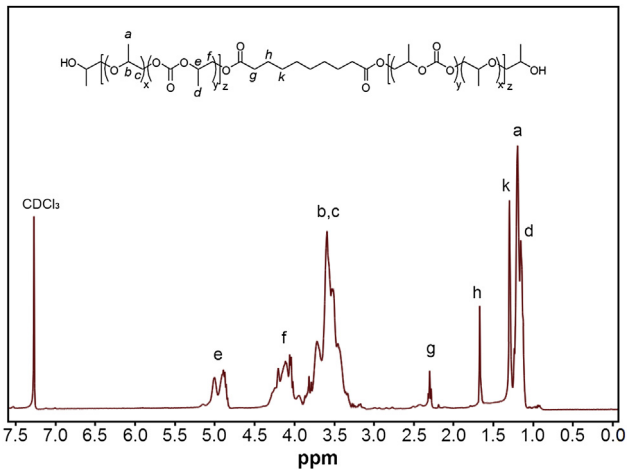

Fig. 1. The molecular structure of poly(carbonate-ether) and its ^{1}H NMR spectrum.

[17]. Herein, a novel polymer electrolyte based on low-molecular weight poly(carbonate-ether) with ca. 30% carbonate unit content and lithium tetrafluoroborate was prepared, the electrolyte system was investigated by FT-IR, AFM and electrochemical measurements. The discharge performance of lithium–oxygen battery fabricated by this polymer electrolyte showed similar cyclic stability compared with tri(ethylene glycol) dimethyl ether/$LiBF_4$ liquid electrolyte.

2. Experimental

Poly(carbonate-ether) (PCE) with number average molecular weight (M_n) of 10 kg mol^{-1} and carbonate unit content of 30% was synthesized by copolymerization of CO_2 and propylene oxide using zinc–cobalt double metal cyanide complex in the presence of sebacic acid [18]. Its molecular structure and ^{1}H NMR spectrum are illustrated in Fig. 1, and its other important properties, such as molecular weight distribution and glass transition temperature, are described in Supporting Information. For polymer electrolyte preparation, a calculated amount of PCE and lithium tetrafluoroborate were dissolved in anhydrous tetrahydrofuran under stirring. After stirring for 24 h within a glove box, the homogeneous solution was cast on a glass substrate, the solvent was removed slowly by an unflagging airflow to form a polymer thin film with

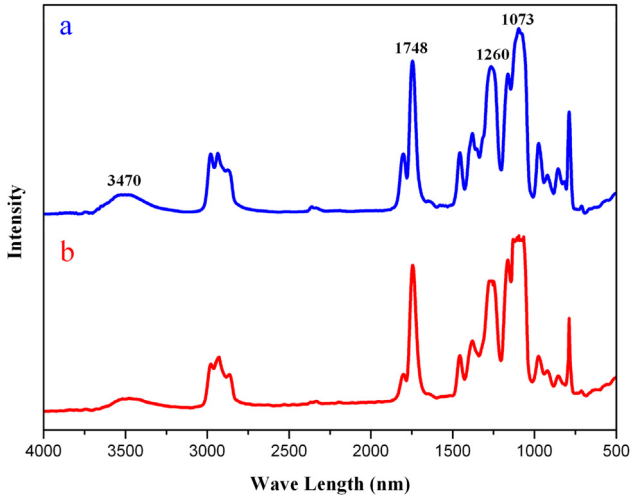

Fig. 2. The FT-IR spectra of pure PCE (a) and PCE/$LiBF_4$ electrolyte with weight ratio of 5:1 (b).

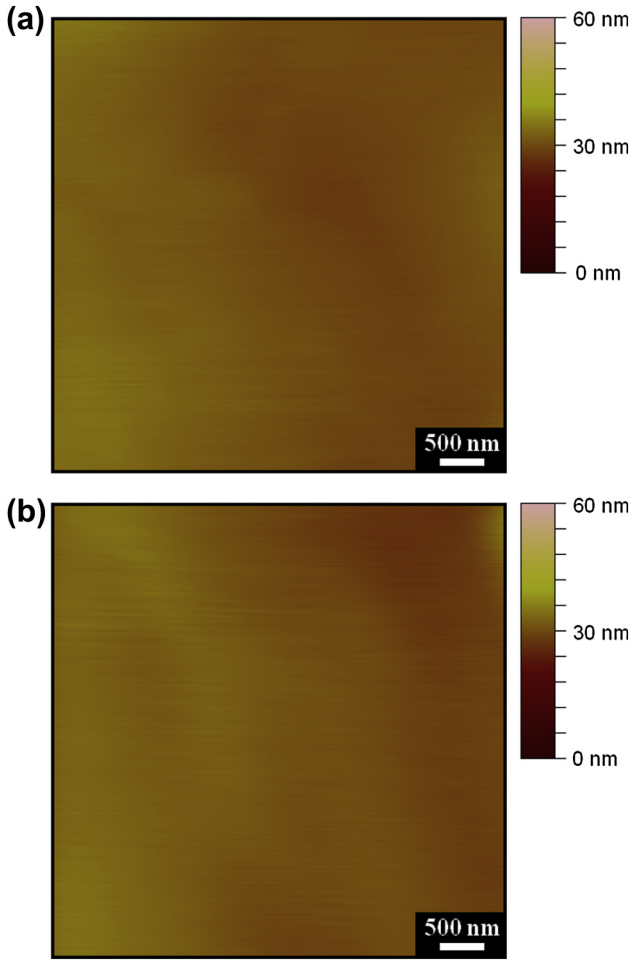

Fig. 3. The tipping-mode AFM images of PCE film surface (a) and PCE/$LiBF_4$ electrolyte film surface (b).

average thickness of 150 μm. Subsequently, the polymer electrolyte film was further dried under vacuum at 100 °C for 48 h.

The Fourier transform infrared (FT-IR) spectra of polymer electrolyte were recorded on a Bruker TENSOR-27 spectrophotometer. The morphology of the polymer electrolyte was observed by atomic force microscopy (AFM, NanoScope IIIA, Digital Instruments, Veeco,

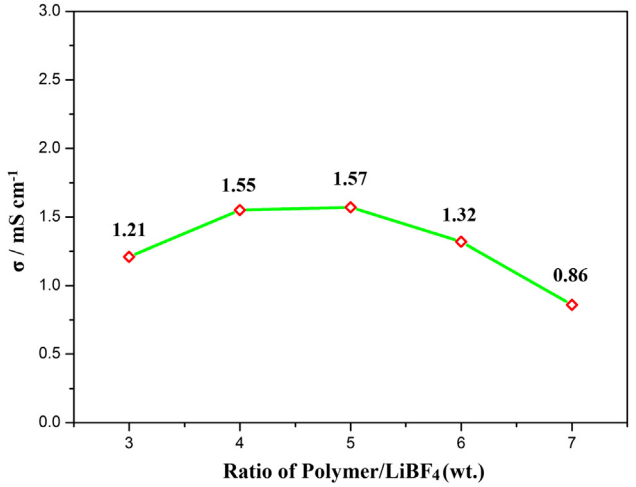

Fig. 4. Dependence of ionic conductivity of polymer electrolyte on weight ratio of PCE to $LiBF_4$.

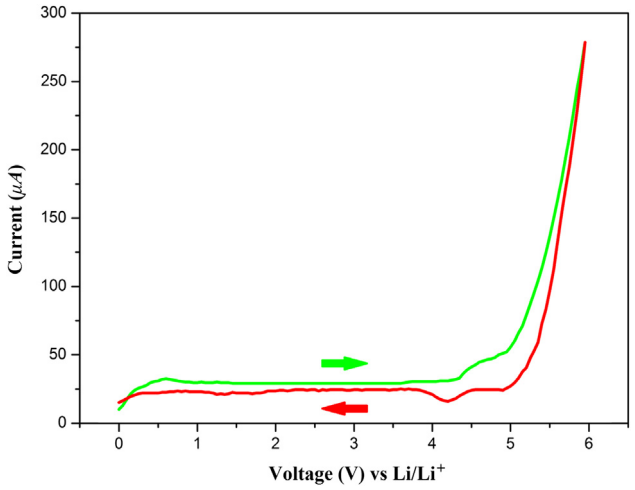

Fig. 5. Voltammogram of PCE/$LiBF_4$ electrolyte vs Li/Li^+. The scan rate was 150 mV s^{-1}.

USA). Evaluation of the electrochemical stability of the polymer electrolyte was carried out by a standard two-electrode system. A lithium thin disk with a stainless steel current collector was used as the counter electrode, and the polymer electrolyte film was sandwiched between the counter electrode and gold working electrode. The voltammogram of this system was measured by Solartron SI 1287 electrochemical workstation under argon atmosphere. The ionic conductivity of the polymer electrolyte was measured by a.c. impedance at frequencies between 50 kHz and 500 mHz at room temperature.

The 2032-type coin cell (schematic illustration showed in Supporting Information) was chosen for the battery electrochemical test. A thin lithium film was used as the battery anode. The polymer electrolyte was placed on it, and a porous polyaniline (PANI) nanofibers cathode (contained 7.5 mg polyaniline) prepared according to our previous work was covered on the top to finish the

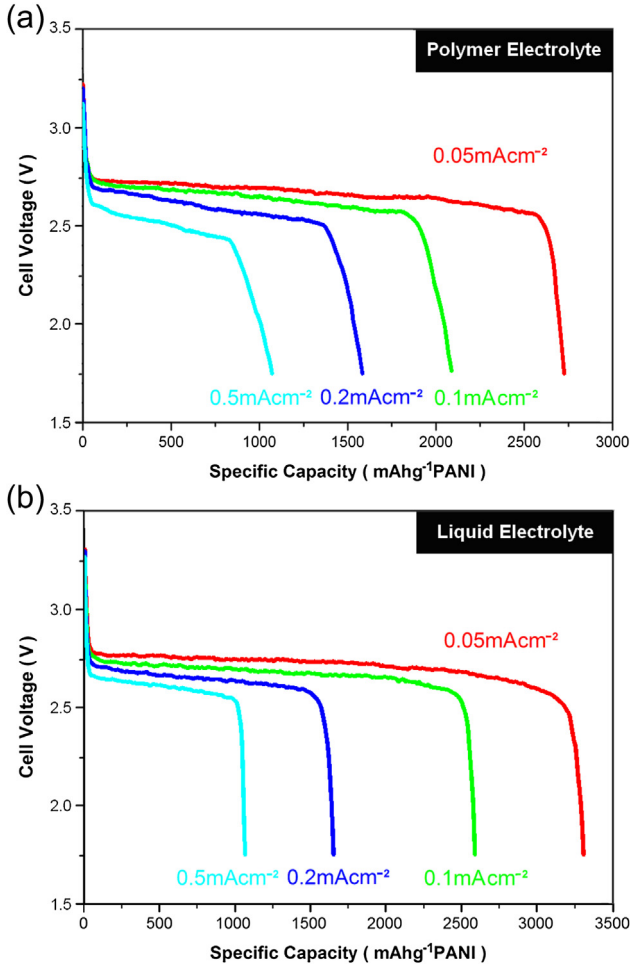

Fig. 6. The discharge curves of the lithium–oxygen battery based on polymer electrolyte and tri(ethylene glycol) dimethyl ether/$LiBF_4$ liquid electrolyte.

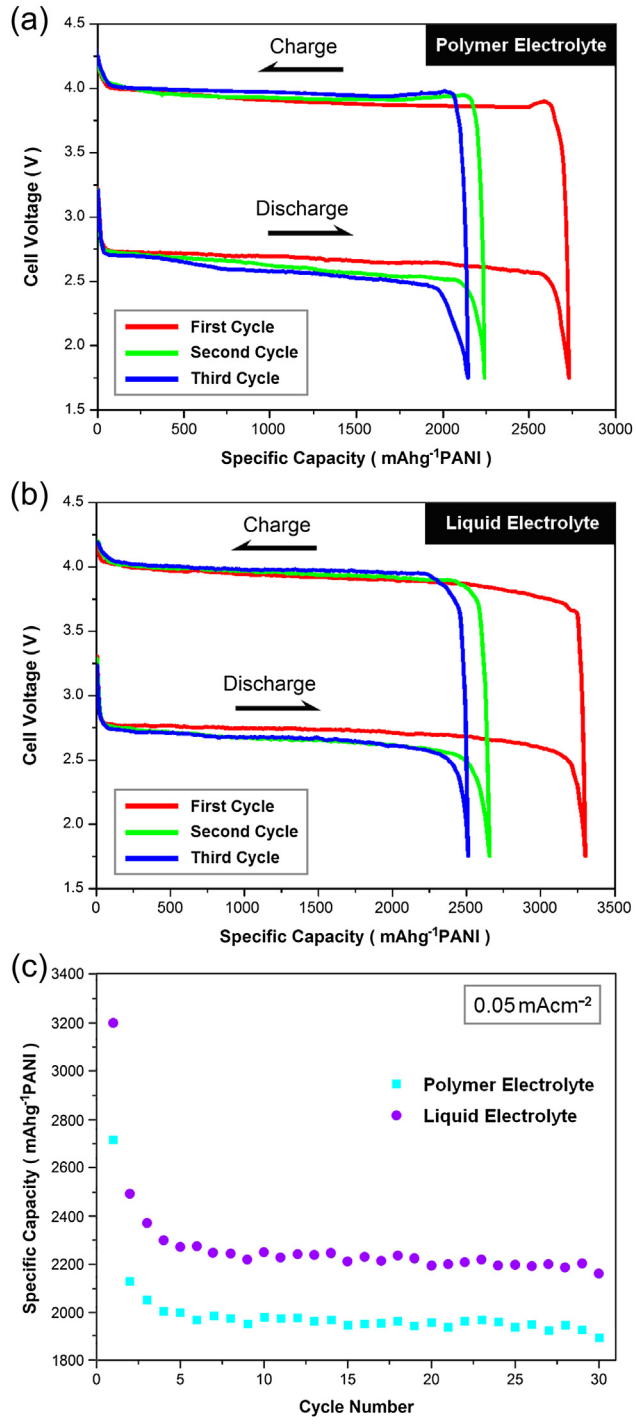

Fig. 7. Charge–discharge curves of the lithium–oxygen batteries based on polymer electrolyte and liquid electrolyte (a) and (b), and the discharge capacities versus cycle number of these two kinds of batteries (c).

battery assembly [19]. For comparison, lithium–oxygen battery was fabricated using tri(ethylene glycol) dimethyl ether/$LiBF_4$ as liquid electrolyte. Their galvanostatic charge and discharge behaviors were recorded on Solartron SI 1287 electrochemical workstation, at different current density within a voltage window between 1.75 and 4.25 V, and all the tests were operated in 2 atm pure oxygen atmosphere.

3. Results and discussion

Infrared spectroscopy was used to study the interaction between the lithium salt and host polymer. The FT-IR spectrum of pure PCE was shown in Fig. 2a. The peaks at 1748 and 1260 cm^{-1} were assigned to the strength vibrations of C═O and C–O in oxycarbonyl groups (–O–C(O)–O) in carbonate segment, respectively, the absorption at 1073 cm^{-1} was assigned to ether linkage in the main chain, and the peak at 3470 cm^{-1} was due to the terminal hydroxyl groups. Obvious changes were observed upon addition of $LiBF_4$, as shown in Fig. 2b where the weight ratio of PCE to $LiBF_4$ was 5:1, the decrease in peak intensity at 3470 cm^{-1} indicated that coordination occurred between the terminal hydroxyl groups of the PCE and the lithium ions. The peak at 1073 cm^{-1} became broad and zigzag, which was a typical mark of the strong interaction between the lithium ions and oxygen atoms in ether segment [20]. The oxygen atoms on both sides of the C═O in oxycarbonyl groups also had interaction with lithium ions, as revealed by the changes of the peak shape and intensity at 1260 cm^{-1}. Instead, the peak at 1748 cm^{-1} assigned to the C═O did not show any obvious change, indicating that there was no interaction between this kind of oxygen atoms and lithium ions.

The morphologies of the PCE film and PCE/$LiBF_4$ composite film (5:1, w/w) were studied by tipping-mode AFM image. As shown in Fig. 3a, the PCE film had very smooth and dense surface, and the height difference was smaller than 60 nm in the area of 5 μm × 5 μm, indicating that the carbonate and ether segments in PCE had very good compatibility and no phase-separation occurred. In Fig. 3b, the PCE/$LiBF_4$ composite film showed a similar surface morphology to the pure PCE. It could not see any small particles on the composite surface, indicating that the $LiBF_4$ had been dispersed evenly into the host polymer. The good miscibility of the lithium salt and the host polymer was very important prerequisite for good ionic conductivity.

The ionic conductivities of the composite electrolytes with various $LiBF_4$ contents were presented in Fig. 4. The composite electrolyte with approximate 17% of $LiBF_4$ gave the highest ionic conductivity of 1.57 mS cm^{-1}, and in that case one lithium ion corresponded to about four ether segments. The ionic conductivity dropped down simultaneously with the decrease of $LiBF_4$ content in the polymer electrolyte. However, the higher $LiBF_4$ content did not bring much higher ionic conductivity, since the excess $LiBF_4$ in the polymer electrolyte failed to provide any contribution to the ionic conductivity due to the reunion phenomenon, instead it blocked the transportation of lithium ions surrounding it [11]. We suppose that the quite high conductivity of this polymer electrolyte is due to its relatively low glass transition temperature compared with its homologues with much higher molecular weight, and more detailed research will be made in our next work.

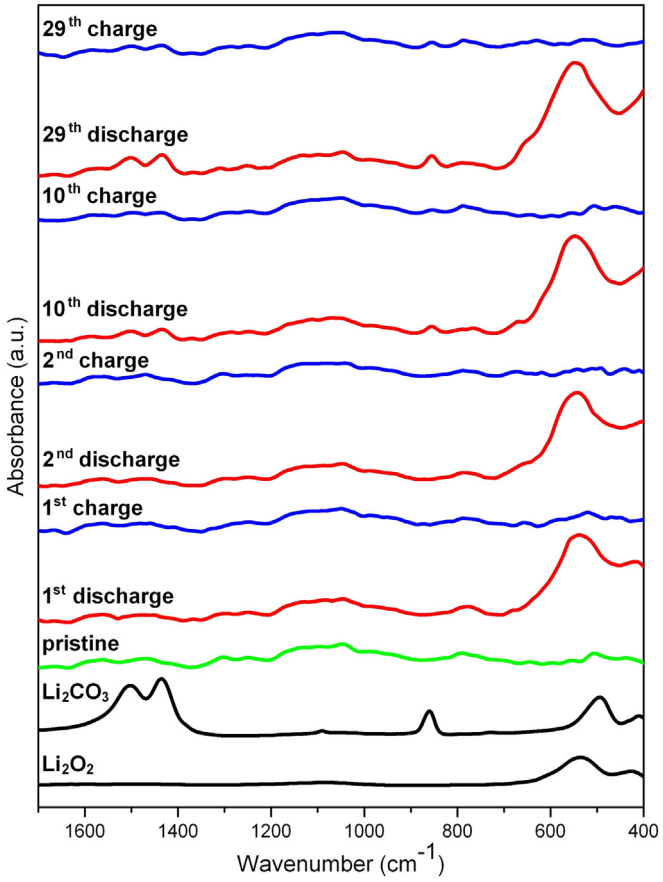

Fig. 8. The FT-IR spectra of polyaniline nanofiber cathode after 1st, 2nd, 10th and 29th charge–discharge cycles.

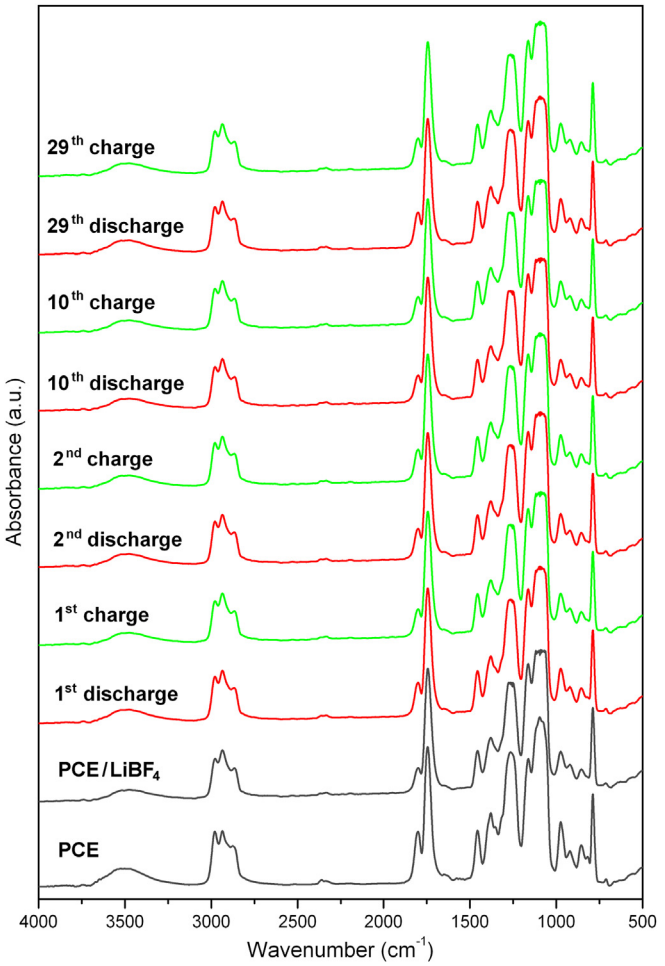

Fig. 9. The FT-IR spectra of the PCE/$LiBF_4$ polymer electrolyte after 1st, 2nd, 10th and 29th charge–discharge cycles.

Polymer electrolyte for lithium–oxygen battery must be chemically stable. Fig. 5 showed the typical voltammogram of the PCE/$LiBF_4$ electrolyte. During the forward scan (from 0 V to 6 V), a small anodic peak at 4.2 V was observed, and this peak was attributed to the decomposition of the polymer electrolyte. However, this polymer electrolyte was electrochemical inert in the potential range of lithium–oxygen battery discharging (below 3.2 V versus Li/Li^+), and the top limits of its electrochemical stability windows was higher than 4.2 V versus Li/Li^+. Therefore, the voltage range between 1.75 V and 4.2 V (versus Li/Li^+) was chosen as the continuous charge–discharge cycling process.

Fig. 6 showed the discharge curves of lithium–oxygen battery based on polymer electrolyte and liquid electrolyte, respectively. At current density of 0.1, 0.2 and 0.5 mA cm^{-2}, nearly all the discharge curves of the lithium–oxygen battery with the polymer electrolyte showed very small difference (<10%) compared with the battery based on liquid electrolyte, indicating that this novel polymer electrolyte could support enough high lithium ion mobility even at high current density of 0.5 mA cm^{-2} in lithium–oxygen battery. However, a quite larger decrease occurred at the current density of 0.05 mA cm^{-2}, it was 3300 mAh g^{-1} PANI for liquid electrolyte, while it dropped to 2730 mAh g^{-1} PANI, nearly dropped by 17.3%, the reason was under investigation.

The galvanostatic charge and discharge curves of lithium–oxygen battery based on the polymer electrolyte and liquid electrolyte were shown in Fig. 7, the current densities were set as 0.05 mA cm^{-2}, and the voltage windows were between 1.75 and 4.2 V. During charge process, the polymer electrolyte still could not help to decrease the excess charging potential, indicating that this battery also had poor charge–discharge efficiency as other kind of lithium–oxygen batteries. The discharge capacity versus cycle number was shown in Fig. 7c. Like the battery based on liquid electrolyte, the discharge capacity of this all-solid-state battery kept relatively stable in the next 27 cycles with only a 7% loss after an initial degradation from 2730 to 2050 mAh g^{-1} PANI during the first three cycles.

In order to further demonstrate the stability of the polymer electrolyte, we also studied the generation-disappearance of Li_2O_2 in the cathode, and the compositional and morphological changes of the polymer electrolyte during the charge–discharge cycles via FT-IR and AFM techniques. In Fig. 8, it showed that the Li_2O_2 generated during each discharge process, and then disappeared during next charge process. Although little Li_2CO_3 began to generate after the 10th charge process, the Li_2O_2 was always the major product of the discharge reaction. In Fig. 9, the FT-IR spectra of the polymer electrolyte after different charge–discharge cycles clearly showed that there was not obvious change on its component. Besides that, AFM images in Fig. 10 showed that the phase-separation did not occur during the charge–discharge cycles, the polymer electrolyte surface kept smooth and even after the 29th battery charging. All of these proved that the polymer electrolyte was stable enough to be employed in lithium–oxygen battery

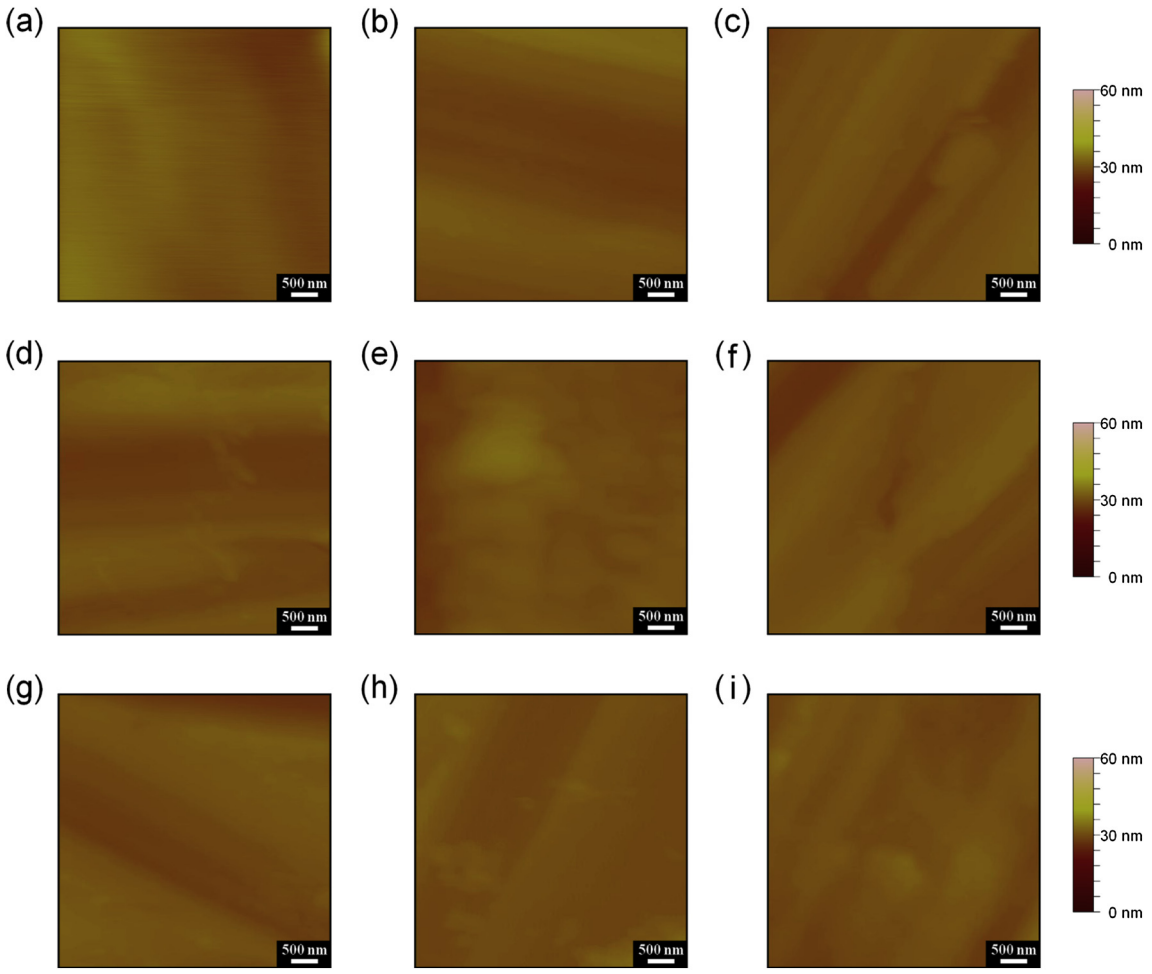

Fig. 10. The tipping-mode AFM images of the initial PCE/$LiBF_4$ electrolyte film surface (a), and its morphology after 1st discharge (b), 1st charge (c), 2nd discharge (d), 2nd charge (e), 10th discharge (f), 10th charge (g), 29th discharge (h), and 29th charge.

system. The initial large degradation of the battery specific capacity should mainly derive from the reunion of the polyaniline nanofibers cathode, and a detailed discussion about this question had been given in our previous report [21].

4. Conclusions

Novel polymer electrolyte based on low-molecular weight poly(carbonate-ether) and lithium tetrafluoroborate was prepared and employed in lithium–oxygen battery for the first time. The electrochemical measurements confirmed that such polymer electrolyte showed similar cyclic stability compared with the battery based on traditional liquid electrolyte, which may provide a new choice for fabrication of all-solid-state high-capacity rechargeable lithium–oxygen battery with better safety. More careful and systematic investigation about the impact of polymer carbonate unit content and molecular weight on the final electrochemical performance of the polymer electrolyte will be reported in our forthcoming paper.

Acknowledgement

This work was supported by the National Science Foundation of China (Grant No. 51021003 and 21134002).

Appendix A. Supplementary data

Supplementary data related to this article can be found at http://dx.doi.org/10.1016/j.jpowsour.2013.05.095.

References

[1] T. Tabuchi, N. Hochgatterer, Z. Ogumi, M. Winter, J. Power Sources 188 (2009) 552–557.
[2] G.R. Dahlin, K.E. Strøm, Lithium Batteries: Research, Technology and Applications, first ed., Nova Science Publisher, Inc., New York, USA, 2010.
[3] V. Etacheri, R. Marom, R. Elazari, G. Salitra, D. Aurbach, Energy Environ. Sci. 4 (2011) 3243–3262.
[4] T. Doi, T. Fukutsuka, K. Takeda, T. Abe, K. Miyazaki, Z. Ogumi, J. Phys. Chem. C 116 (2012) 12422–12425.
[5] J. Christensen, P. Albertus, R.S. Sanchez-Carrera, T. Lohmann, B. Kozinsky, R. Liedtke, J. Ahmed, A. Kojic, J. Electrochem. Soc. 159 (2012) R1–R30.
[6] P.G. Bruce, S.A. Freunberger, L.J. Hardwick, J.M. Tarascon, Nat. Mater. 11 (2012) 19–29.
[7] G. Girishkumar, B. McCloskey, A.C. Luntz, S. Swanson, W. Wilcke, J. Phys. Chem. Lett. 1 (2010) 2193–2203.
[8] J. Xiao, D. Mei, X. Li, W. Xu, D. Wang, G.L. Graff, W.D. Bennett, Z. Nie, L.V. Saraf, I.A. Aksay, J. Liu, J.G. Zhang, Nano. Lett. 11 (2011) 5071–5078.
[9] S. Ida, A.K. Thapa, Y. Hidaka, Y. Okamoto, M. Matsuka, H. Hagiwara, T. Ishihara, J. Power Sources 203 (2012) 159–164.
[10] E. Yoo, H. Zhou, ACS Nano 5 (2011) 3020–3026.
[11] D. Zhang, R. Li, A. Yu, J. Power Sources 195 (2010) 1202–1206.
[12] B.B. Owens, J. Power Sources 90 (2000) 2–8.
[13] A.M. Stephan, Eur. Polym. J. 42 (2006) 21–42.
[14] M.M. Silva, S.C. Barros, M.J. Smith, J.R. MacCallum, Electrochim. Acta 49 (2004) 1887–1891.
[15] D.J. Darensbourg, Chem. Rev. 107 (2007) 2388–2410.
[16] G.W. Coats, D.R. Moore, Angew. Chem. Int. Ed. 43 (2004) 6618–6639.
[17] G.P. Wu, S.H. Wei, W.M. Ren, X.B. Lu, T.Q. Xu, D.J. Darensbourg, J. Am. Chem. Soc. 133 (2011) 15191–15199.
[18] Y. Gao, L. Gu, Y. Qin, X. Wang, F. Wang, J. Polym. Sci. Part A: Polym. Chem. http://dx.doi.org/doi:10.1002/pola.26366.
[19] H. Zhang, Q. Zhao, S. Zhou, N. Liu, X. Wang, J. Li, F. Wang, J. Power Sources 196 (2011) 10484–10489.
[20] M.J. Reddy, P.P. Chu, U.V.S. Rao, J. Power Sources 158 (2006) 614–619.
[21] Q. Lu, Q. Zhao, H. Zhang, J. Li, X. Wang, F. Wang, ACS Macro Lett. 2 (2013) 92–95.